Design and Realization of Stretchable Sewn Chipless RFID Tags and Sensors for Wearable Applications

Arnaud Vena, Elham Moradi, Karoliina Koski, A. Ali Babar, Lauri Sydänheimo and Leena Ukkonen
Department of Electronics, Rauma Research Unit
Tampere University of Technology
Finland
arnaud.vena@tut.fi

Manos M. Tentzeris
School of ECE
Georgia Tech, Atlanta, GA 30332-250
USA
etentze@ece.gatech.edu

***Abstract*—This paper presents the design of a sewed chipless RFID tag and sensor, on a fabric for wearable applications. The proposed design is based on three sewn scatterers on cotton textile. The tag is realized using a computer-aided sewing machine and electro-thread plated with silver. The simulation and frequency-domain measurement results validate the design from 3 to 6 GHz. The tag's static backscattered response can be identified in free space and on the human body. Some preliminary results from a sewn stretchable sensor are also given to demonstrate the potential for biomedical applications. Finally, we discuss the main challenges concerning the practical implementation of this technology.**

Keywords—RFID; chipless RFID; fabrics; embroidery; stretchable; sensor; scatterer; UWB

I. INTRODUCTION

The RFID technology is currently used in thousands of different applications [1]. Mainly, the applications of pallet tracking and identification of persons and animals have largely adopted this technology. Additionally, wearable RFID technology is gaining more interest every day with a great potential in the fields of WBAN and on-body health tracking as reported in previous works [2-10].

On-body RFID technology can be achieved by several realization techniques. A simple way is to realize tags based on conventional etching techniques on commonly used substrates and then to embed them into a dielectric [8]. This overall assembly can then be integrated into clothes. However, in terms of cost and its durability in washing and mechanical stresses, the use of conductive fibers is considered promising. Moreover, this technology allows seamless integration of antennas with clothes. An innovative technique relies on sewing the tag antenna directly on garments. For this purpose, one can use conductive yarns as reported in [3;6;7;10].

However, the main drawback of sewn tags is still the connection between the antenna and the chip. Typically, conductive adhesive connects threads to chip electrodes, but the mechanical robustness of this assembly is weak. Some new ideas are emerging to overcome this critical issue. A small loop antenna can be connected to a chip IC in a first stage. This assembly is then placed at the center of a sewn antenna to feed it by coupling effect [9]. In the present case, we utilize stretchable fabrics. Thus, this last technique cannot be implemented because the quality of the coupling depends on the electric length variation of the conductive strip. This leads to lower the radiation efficiency compared to a direct electrical connection between the chip and the antenna.

For several years, chipless RFID [11-19] is under investigation mainly to decrease the cost of tags to address consumer goods market. This market is still today primarily dominated by the optical barcode technology [20]. Not only, for its lower cost, may the chipless RFID technology bring some improvements for certain applications that don't require a large coding capacity such as for sorting objects (banknote, coins, tokens…). Firstly, there is no chip, so no complex and costly operation is required to connect a chip to an antenna. The chipless technology can work in harsh environment such as high pressure, high temperature or abnormal radiation level environment. A sewn tag can be integrated with clothes nearly for free and can serve as a first level anti-theft system for clothing brands or in an automatic laundry for identification of clothes. A chipless tag is a combination of one or several

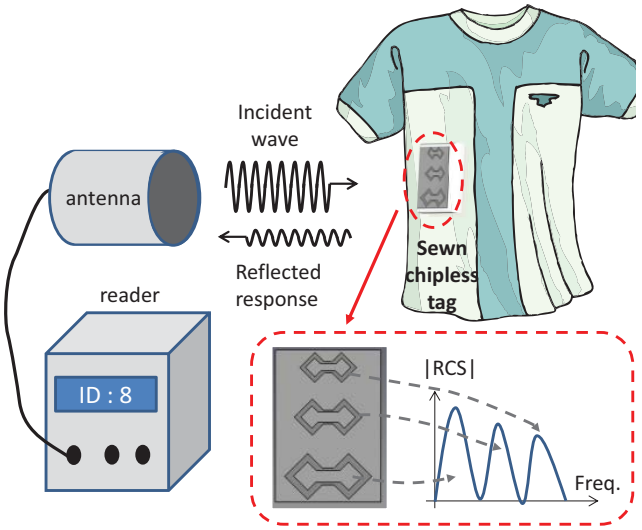

Figure 1. Chipless RFID system for wearable applications.

978-1-4673-5750-0/13/$31.00 ©2013 IEEE

antennas and/or other resonant structures (see Fig. 1). They usually require only one conductive layer so that low-cost printing process can perfectly realize an entire chipless tag or sensor with no more operations [21].

This work focuses on the design and the realization of a sewn chipless tag. It has been motivated by the fact that its realization is simpler than a conventional RFID tag. Section II will recall the basic principles of the chipless RFID technology. Then in section III, a design will be proposed to operate efficiently for the relatively low conductivity achieved with the electro–threads. We present in section IV a concept of sewed chipless sensors for monitoring the stretching of objects or humans. Finally, we discuss the practical implementation challenges of this novel technology; transmitted power regulations and on-body detection.

II. CHIPLESS RFID PRINCIPLES

The way to extract an identifier (ID) from the tag is fully different compared to a conventional tag. There is no communication protocol and modulation of a continuous-wave signal. A chipless tag doesn't embed any power recovery system or transceiver. It is a fully passive circuit. The analysis of the impulse response of the tag excited by an incident plane wave is the only way to identify the tag. The radar cross section (RCS) is a parameter to characterize the level of reflectivity of a radar target, in this case the tag. The RCS can be extracted as a function of the incident angle of the transmitted signal and depends on the frequency. Different techniques of coding have been used to make the link between a given EM signature and a unique ID. Some techniques are based on the time-domain analysis on the impulse response. The other ones use an ultra-wide band (UWB) frequency analysis.

A simple and reliable coding technique is related to the presence or the absence of peaks or dips at several frequency points [13]. In this case, one bit is equal to one resonant peak. In this paper, the simple absence / presence coding technique has been used for wearable prototypes realized with electro-threads. It has to be noted that the conductivity of a sewn strip is relatively low, (about 3000 S/m for the pattern used), so the quality factor of scatterers can generate a frequency peak with a large bandwidth that could potentially limit the frequency resolution of the detection system.

III. SEWN CHIPLESS RFID TAGS

A. Realization process and Material characterization

The tag design has been optimized based on the fabric substrate parameter and the conduction losses of metallic threads. The two fabrics used in this study are cotton and synthetic stretchable textiles. Their features are given in Table I. The complex permittivity has been extracted using the Agilent dielectric probe kit 85070E.

The electro-threads used are Shieldex 110f34 dtex 2-ply HC [22]. The thread is based on 34 filaments plated with silver. A single thread of 160 µm diameter has a DC linear resistivity of 500 Ω.m ± 100 Ω.m. To realize a sewn conducting strip, tens of threads are involved. For DC frequency, a model based on several parallel resistances may allow getting a close resistance value of the strip. For radio-frequencies, a simple model cannot be extrapolated due to the skin effect and the coupling effect between each thread. Moreover, as shown in [3;6], the RF conductivity can vary a lot depending on the sewing pattern. However, a study stated in [6] shows that a simple model of a sewn strip can be adopted in a full wave simulator. A sewn strip can be approximated by an effective bulk conducting strip having the same dimensions as the pattern. The conductivity varies between 10^3 S/m and 10^4 S/m depending on the sewing pattern. The main parameters affecting the conductivity are the density of stitches per surface unit and the orientation of the threads. When the threads are aligned along the surface currents, the conductivity is maximized. The textile features show quite significant losses, but it is electrically thin, thus the overall losses will be mostly affected by the conductive losses. To realize the chipless tag, a computer-aided sewing machine is used. This is a Husqvarna Viking machine able to sew with a resolution of 1 mm. This resolution determines the upper frequency limit and the frequency resolution (70 MHz at 3 GHz, 250 MHz at 6 GHz, 700 MHz at 10 GHz) achievable regarding a frequency domain encoding technique.

TABLE I. FABRIC FEATURES

Fabric	***Stretchable polyester***	***Cotton***
Thickness	1 mm	0.25 mm
ε_r @ 1GHz	1.4	2.2
Tanδ @ 1GHz	0.022	0.07
ε_r @ 2GHz	1.4	2.1
Tanδ @ 2 GHz	0.022	0.07

B. Optimized Tag Design

Based on the aforementioned material characteristics, a design for an individual scatterer has been put together for a 300-400MHz bandwidth within the UWB band of 3-6GHz. The tag shown in Fig. 2 (a) and (b) is made of dual rhombic loop scatterers [23-24]. The width of strips is important, about 4 mm to decrease the resistance effect and increase the radiation efficiency. The shape describes a closed loop. The Fig. 3 (a) and (b) show the electric field distribution and the surface currents distribution respectively. Surface currents intensity (in Fig. 3 (a)) is maximum near the left and right edges and minimum at the center of the loop. Moreover, the electric field in Fig. 3 (b) is maximum at the center of the loop. Thus, the first resonant mode appears when the wavelength is equal to half of the total length of the loop. The "diamond-shape" rings at the two edges of the scatterer allow for the increased RCS while the narrower strip spacing in the middle of the loop enhances the scatterer's selectivity.

This scatterer has been optimized around the center operating frequency of 4.5 GHz based on length, width strip, height of the diamond-shape ring and central strip spacing. The conductivity value used in the simulated model for the chosen sewing pattern shown in Fig. 2 (c) is 3000 S/m for a thickness of 100 µm. As a result, a resonant peak with a RCS close to -25 dBsm and a 3 dB bandwidth of 400 MHz are obtained, which is a quite satisfactory performance considering the low conductivity value of the strips. The composite effect of the

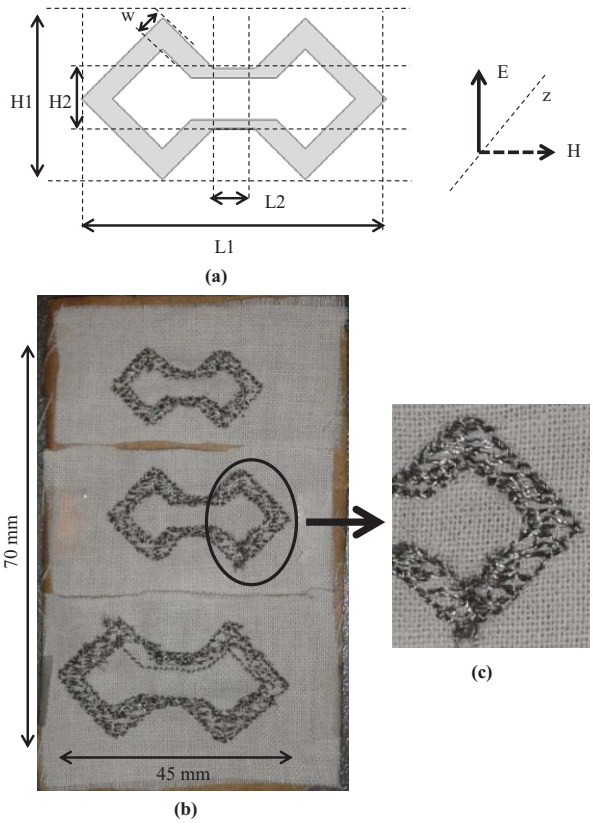

Figure 2. (a) Dual rhombic loop scatterer (b) Sewn Chipless RFID tag design based on 3 dual rhombic loop scatterers. (c) Magnified view of the sewn pattern

chipless tag will cover the chosen UWB range; the structure will be composed of numerous 400 MHz resonators based on the bit number we want to include. Fig. 4 presents the RCS simulation results obtained with CST Microwave Studio. It can be seen that the strip width has a great influence on both the RCS and the resonant frequency. As stated earlier, a large strip width has to be preferred for increased RCS. The resonant frequency varies because the inductance of the rings is correlated with the strip width.

Based on the scatterer optimization, a chipless tag can be designed. In this study, three scatterers are used to generate three resonant peaks from 3.5 GHz to 6 GHz. Each peak is located in a frequency span of 800 MHz to limit the overlapping of their EM response and ease their detection. Based on absence / presence coding technique, eight different IDs or 3 bits can be encoded. The chipless tag is composed of multiple similar scatterers designed around different resonant

TABLE II. SCATTERERS DIMENSIONS IN MM

Resonant Frequency	*L1*	*L2*	*H1*	*H2*	*W*
3.5 GHz	41.5	5.6	22.1	8.2	4
4.8GHz	32.4	4.4	17.2	6.4	3
6GHz	27	3.7	14.4	5.4	2.5

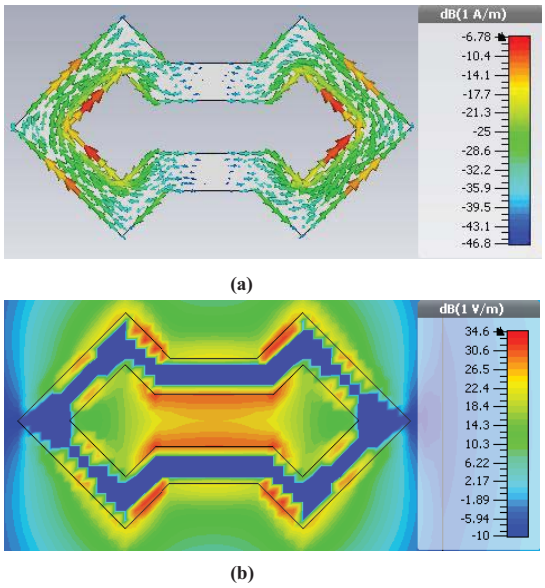

Figure 3. (a) Surface currents distribution and (b) electric field distribution of the dual rhombic loop scatterer, at the resonant frequency, excited by a plane wave. These results have been obtained with the help of CST Microwave Studio.

frequencies (between 3 and 6 GHz). The dimensions of the three realized scatterers are given in Table II.

C. Measurements results

To measure the RCS of the sewn tag a frequency-domain measurement setup has been used. This measurement principle relies on the mono-static continuous-wave (CW) radar frequency sweep already investigated in [16]. It is composed of a vector network analyser (VNA) Agilent PNA E8358A. The two ports of the VNA are connected to a dual polarized wide-band antenna ETS Lindgren 3164-04 with a gain between 9 dBi and 12 dBi between 3 GHz and 6 GHz. The vertical

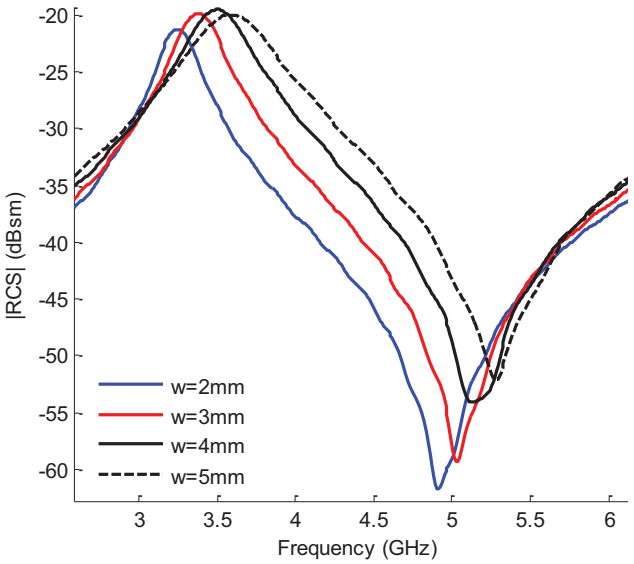

Figure 4. |RCS| Simulation results for a sewn dual rhombic loop scatterer obtained with the help of CST Microwave Studio. The dimmensions of the scatterer are given Table II, first row.

polarization input of the antenna is connected to the port 1 of the VNA, while the port 2 is connected to the horizontal polarization input. The record of the parameters S11 and S22 will provide information about the backscattered signal for the vertical polarization and for the horizontal polarization, respectively. A calibration procedure described in [16] is used to extract the RCS value from raw measurements. It is based on 3 successive measurements:

The "vacuum" (no "scatterer" present) environment.

The EM response of a reference scatterer.

The tag EM response.

A picture of the measurement set-up is shown in Fig. 5 (a) and (b). As one can see, the tag is placed on a polystyrene stand at 20 cm away from the horn aperture. The measurement environment is an office with furniture such as tables having metallic feet, and surrounding wireless communications systems such as cell phone and Wifi networks. Thus, the chipless tag response has to be extracted among all these interfering signals. A chipless tag is a static radar target and generates, every time, perfectly the same EM signature for the same distance and angle of illumination. The surrounding wireless communications can be considered, for a long integration time, as uncorrelated signals compared to the tag response. By applying averaging on tens of repetitive measurements, the EM signature of the tag can be extracted. Equation (1) can be used to extract the frequency sample k of the average tag response $Tagresp_{ave}$ based on N similar measurements denoted $Tagresp_i$. The additional term $Srf_i(k,t)$ represents the effect of the surrounding noise. In the case where the interfering signals are considered uncorrelated regarding the tag response recording time, equation (2) can be used in which the mean of $Srf_i(k,t)$ becomes null. The results shown in Fig. 6 and Fig. 7 have been carried out based on an averaging with N=20 measurements. This number is enough to get a significant EM tag response for a range of 20 cm as shown in Fig. 6. To operate with a greater range the number of repetitive measurements, N, could be increased. It is noteworthy that this choice affects the signal to noise ratio (SNR).

$$Tagresp_{ave}(k) = \sum_{i=1}^{N} \frac{Tagresp_i(k)}{N} + \sum_{i=1}^{N} \frac{Srf_i(k,t)}{N} \quad (1)$$

$$Tagresp_{ave}(k) \approx \sum_{i=1}^{N} \frac{Tagresp_i(k)}{N} \quad (2)$$

Figures 6 and 7 show respectively the RCS magnitude and the phase of the backscattered signal from 3 GHz and 6 GHz. The three scatterers generate the three resonant peaks. The curve in which the three peaks are visible is generated by the tag with the binary ID '111'. Additional measurements have been carried out for several configurations in which some of the scatterers are missing. When the largest one is removed, only two resonant peaks at 4.7 GHz and 5.5 GHz can be observed, and the ID '011' is generated. Inversely, if the smallest one is removed, solely the two first peaks can be seen, giving the ID '110'. The phase measurement in Fig. 7 confirms this behavior and can enhance the reliability for peak detection.

(a) (b)

Figure 5. View of the mono-static CW frequency sweep radar measurement system. (a) Front view. (b) Side view.

Indeed, if the three scatterers are present, three notches can be observed while only two notches are observed when one of the scatterers has been removed. It is important to note that the three scatterers are uncoupled because the resonant frequencies are independent of the configuration. However, the EM response detected by the measurement system relies on additive and destructive interferences created by the complex summation of each scatterer EM response. This explains the phase variation observed in Fig. 7 for the first resonance mode. The three tags encoding the ID "111", "110" and "101" should present the same phase value for the first mode but due to interferences, this is not the case. At least, the phase shape of these three configurations is correlated unlike those of the tag with the ID "011". This finally provides improved detection reliability. These measurements prove that a sewn tag realized on cotton fabric can be detected in a real environment, at least in free space, among many interfering signals. The following part will present a concept of a chipless sensor sewn on stretchable fabric. Practical issues concerning the allowed transmitted power restrictions and the feasibility of on-body measurements will be treated in the last part.

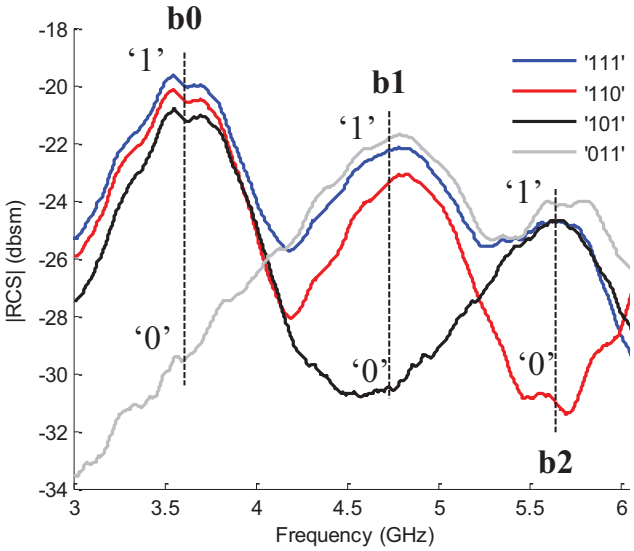

Figure 6. |RCS| Measurement results for several tag configurations.

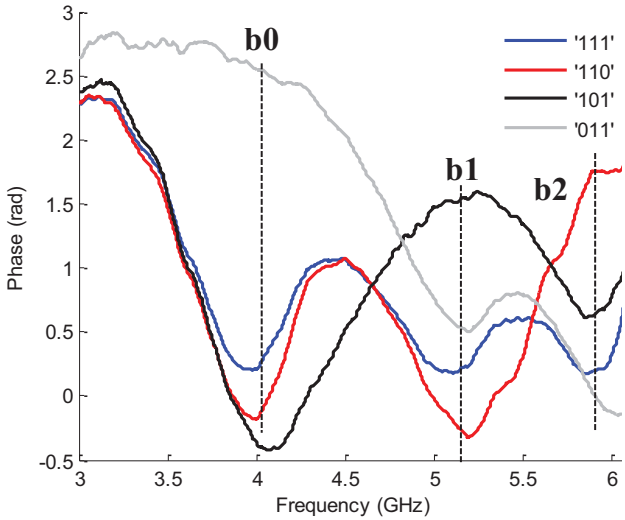

Figure 7. Phase measurement results for several tag configurations.

Based on the measurement results obtained (RCS values) we can extrapolate the theoretical read range using the radar equation in (3).

$$R^{\max} = \sqrt[4]{P_{tx} \cdot Gtx.Grx \cdot \frac{\lambda^2}{(4 \cdot \pi)^3 \cdot P_{rx}^{\min}} \cdot \sigma_{\min}} \quad (3)$$

The calculated value depends on the transmitting power P_{tx}, the gain of the transmitting antenna G_{tx}, the receiver sensitivity P_{rx}^{min}, the gain of the receiving antenna G_{rx}, the minimum RCS level σ_{min} that we wish to detect. Additionally, the receiver sensitivity depends on several measurement settings. For our measurement set-up, we used a VNA. The sensitivity of the receiver could be defined equal to the noise level. This noise level could be minimized depending on both the IF filter and the averaging factor used. A sensitivity of P_{rx}^{min} =-80 dBm can be achieved, with an IF filter of 1 kHz and an averaging factor of 20, in a practical environment (indoor). The maximum stabilized transmitting power is P_{tx}=10 dBm. The gain G_{tx}, G_{rx} of our antenna is around 10 dBi. Based on (3) we can extrapolate the value of the theoretical read range that it can be achieved. According to the measured results in Fig. 6, the minimum RCS value is σ_{min}= -32 dBsm for the 3 bits chipless tag. The read range is related to the maximum operating frequency (6 GHz). Finally we obtain R_{max}=1.68 m.

IV. Toward a Sewn Chipless Sensor

A. Concept and sensor Design

Based on these promising results, we apply the concept of sewn chipless tag to realize a sensor. Chipless sensors are attracting growing interest because they can provide accurate and repeatable results compared to conventional RFID sensors, where the chip versatility has a strong influence on results.

RFID technology for biomedical applications is a hot topic. Thus, it is convenient to study a concept of wearable chipless sensors even if it appears really challenging. The main reason is due to the body effects on the tag's EM response. This will be discussed later in the part V.

In the following study, we aim to design and realize a sewn chipless sensor on a stretchable fabric. The idea is to realize a force, a weight or a strain sensor in a very simple and low-cost way. For this purpose, a polyester fabric has been used. Its features are given in Table I. The realization process based on the use of conductive thread is perfectly adapted for this application because threads are really flexible and resistant to straining. The single scatterer of the Fig. 8 (a) has been designed and realized in order to obtain a frequency shift as a function of the stretching of the fabric. When a pulling force is applied to the fabric, the scatterer length is increased along the applied force axis. Because the resonant frequency of a loop shaped scatterer (see Fig. 8 (a)) is directly linked to its length, a direct relation between the applied pulling force (or the stretching), and the resonant frequency of the scatterer can be obtained. It is notable that stretching the fabric, results in an effective permittivity decrease of the substrate that may affect the resonant frequency. However, this effect is not significant compared to the electrical length increase of the strips.

We designed the scatterer of the Fig. 8 (a) for operating frequencies close to 1 GHz. It was not aimed in this case to make a sensor compliant with the power regulation rules. This experiment should be considered as a preliminary work that can be optimized to operate within UWB frequencies.

B. Results

The RCS has been measured in a real environment with the same setup as the one introduced in part III.C. In order to stretch the fabrics, simple pins have been used as shown in Fig. 8 (b). Before each measurement, the length dimension has been noted. When no pulling force is applied to the sensor, the scatterer length is equal to 88 mm. Several forces have been

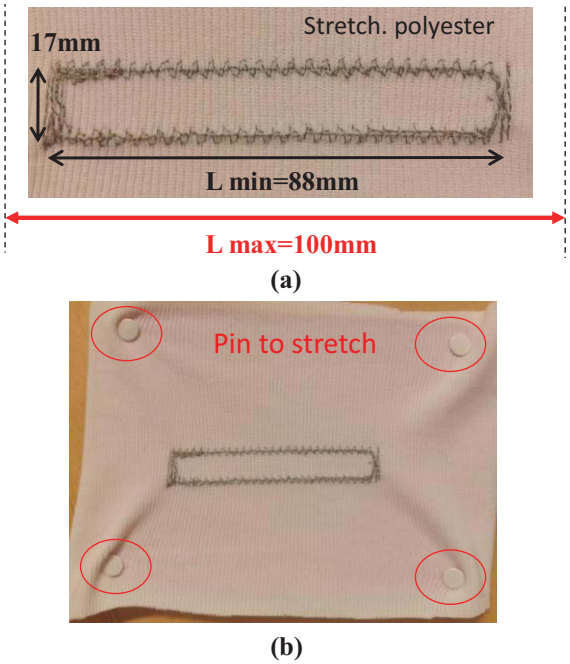

Figure 8. Picture of the sewn scatterer on the stretchable polyester fabric.

applied to extend the length until 100 mm. Figure 9 shows the measured RCS for each corresponding stretching. A resonant peak between 1.2 GHz and 1.4 GHz can be clearly seen and a large frequency shift close to 150 MHz is measured between the minimum and the maximum length.

The RCS level tends to decrease when the stretching rise except for the length 96mm. This effect is due to positioning inaccuracy when setting the tag on the stand after each new stretching. However, the resonant frequency is not affected. Based on these records, a relationship between the length and the peak frequency is extracted and shown in Fig. 10. One can see that from 1.2 GHz to 1.4 GHz, the linear equation (4) can approximate the measured frequency shift. The length L in mm related to the stretching is calculated as a function of the resonant frequency f_0 in GHz as:

$$L = -82.6 \cdot f_0 + 203.1 \quad (4)$$

These results confirm that stretchable fabrics and conductive thread can make accurate chipless sensor even for simple shaped structures such as the rectangular loop of the Figs. 8 (a) and (b). During the measurement, the thread didn't break, so implying that the sensor is mechanically robust. Of course, once again, these measurements have been driven in a real office environment in free space.

V. Discussion and Drawbacks

The previous parts have shown that a chipless RFID tag or sensor can be realized on fabrics and detected in free space. The RCS magnitude makes the tag detectable, but the quality factor of resonators is low, so that a 3 dB bandwidth close to 400 MHz can be achieved based on a conductivity of 3000 S/m. Until now, the measurements of chipless RFID tags have been carried out in free space with no object below; the most favorable conditions for the tag. The detection system requires a large frequency span in which we are not allowed to send that much power (0 dBm). However, it is noteworthy that

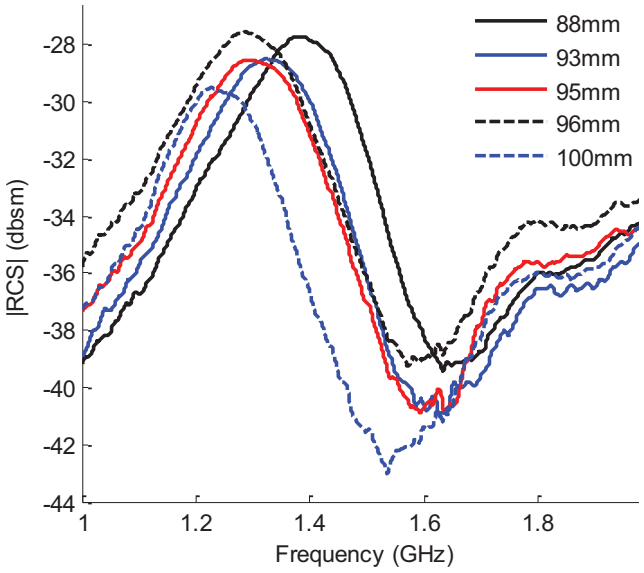

Figure 9. |RCS| Measurement results for several stretching.

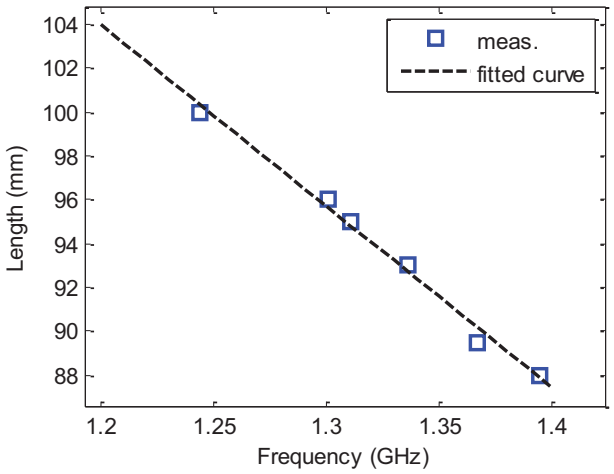

Figure 10. Extracted relationship between the resonant frequency shift and the length increase of the scatterer.

all the results shown throughout this paper have been obtained in a real office environment. This means that the tag is detected among many wireless communication systems such as the Wifi network and, in surrounding with many metallic objects having an RCS much higher than the tag itself. This has been achieved thanks to the records of several repetitive measurements for which an averaging filter has been applied.

A. Radiofrequency Transmitting Power Issues

The main drawback of chipless RFID from a general point of view is that it requires a UWB frequency span to allow identification of tags. The sewn tag designed in this paper operates between 3.5 GHz and 6 GHz, meaning that FCC rules concerning UWB communication systems have to be applied for this purpose. The rules are constraining for CW systems. Only a transmitting power spectral density (PSD) of -41.3 dBm/MHz is allowed. However, one of the promising solutions consists in using impulse radio UWB systems [25]. This allows sending a large instantaneous power within a short duration. The system is compliant regarding the PSD limit because the signal has a very low duty cycle, so the average power is not significant. On the other hand, a system performing polarization diversity with a dedicated chipless tag [18], could be an alternative to the transmitting power issues. In that situation, it can work within several ISM bands. Further, the surface absorption rate (SAR) has to be considered when dealing with on-body applications. The transmitting power for UWB systems is very weak so that this is probably not an issue to detect a chipless tag on the human body. However, this topic has not already been investigated and could be investigated in a future work.

B. On body detection

It is obvious, that for wearable applications, the on-body operation of chipless tags has to be considered. It is already hard for a conventional RFID, for which read range of 1.3 m can be achieved [10]. It is even more challenging for chipless technology for which the RCS of the tag is usually much lower than the RCS of the human itself. The weak tag response is overlapped by the strong body response. Moreover, human

body is usually mobile and its RCS is changing every time. The breathing makes the RCS change. However, if the chipless tag is placed a little away (1–2 cm), it can be shown that the losses due to the human body conductivity are not predominant. Thus, the tag EM response can be detected provided that the signature of the body is filtered. For this purpose, the body RCS has to be recorded firstly and then subtracted from the body plus the tag response. Therefore, it seems to be nearly impossible to detect a tag remotely on a moving body and within a large detection area. However, for short-range operation, it becomes feasible. In this case, a part from the body such as an arm has to be placed in narrow detection area at a given distance from the antenna. Hence, the RCS of the arm is almost the same for each reading. Another solution may consist in using a narrow beam antenna, to get only reflection from a small body area, and the tag located inside this area.

Figure 11 (a) shows the simulation setup used to study the effect of the body on the EM response of a dual rhombic loop scatterer. For this purpose, a lossy dielectric can roughly approximate the local effect of the human arm on the scatterer radiation based on a simple body model experimented in [26]. The arm model is made of two layers: a 3 mm thick skin + fat layer and a 20 mm thick muscle layer. The first one is modeled with εr=14.5 and σ=0.25 S/m, and the second one with εr=55.1 and σ=0.93 S/m. Figure 12 shows simulation results for the dual rhombic loop scatterer when it is placed from 0 mm to 20 mm away from the arm model. If a subtraction is made between the arm response and the total response of both the scatterer and the arm, a resonant peak can be observed in the spectrum as shown in Fig. 12. The scatterer generates a peak frequency at 3.5 GHz in free space. For a separation of 7.5 mm and 10 mm, resonant peaks can be observed but the frequency is shifted between 3.3 GHz and 3.4 GHz. Finally, for a separation of 20 mm, we observe a resonant frequency of 3.5GHz. These simulation results confirm that detection of a sewn chipless tag on-body is possible for close range operation. A separation at least superior to 7.5 mm between the tag, and the body is mandatory. To validate this assumption, we carried out on-body measurements as shown in Fig. 11 (b). We measured the scatterer of the Fig. 11 (a) placed on foam 20 mm

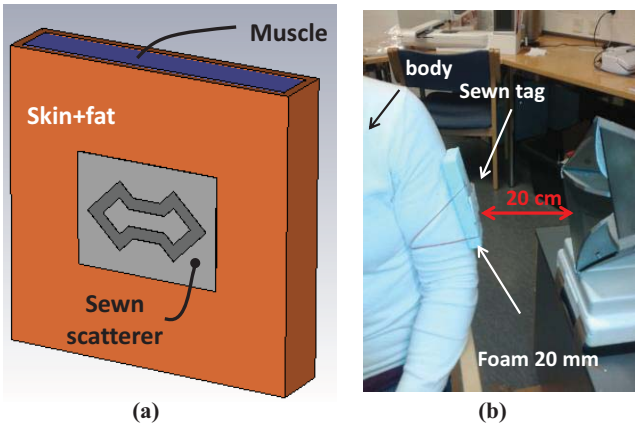

Figure 11. (a) Simulation set-up for a dual rhombic loop scatterer close to a lossy and conductive dielectric. (b) Measurement set-up for on-body detection.

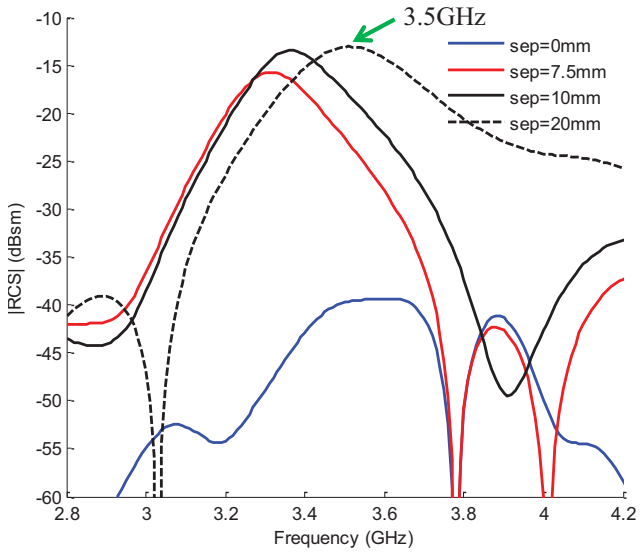

Figure 12. Simulation results of a dual rhombic loop scatterer close to a lossy object. These results have been obtained after having made a subtraction between the lossy object response alone and the total response with the scatterer.

thick as shown in Fig. 11 (b). The assembly is putted on the left arm. The distance between the tag and the aperture of the antenna is 20cm. To compensate the RCS variations due to the movements of the body, we found that an averaging from 30 to 40 records is enough to extract the tag's response. It is noteworthy that, to compensate the movement of the body efficiently, each record has to be quick to compare with the rate of variation of the RCS. So typically we used an IF Bandwidth of 10 kHz to allow for a fast measurement. The measurements results shown in Fig. 13, confirm that the on-body response is well correlated with the free space response. The curve shape varies a few around the resonant peak, but its height and its resonant frequency can be recovered.

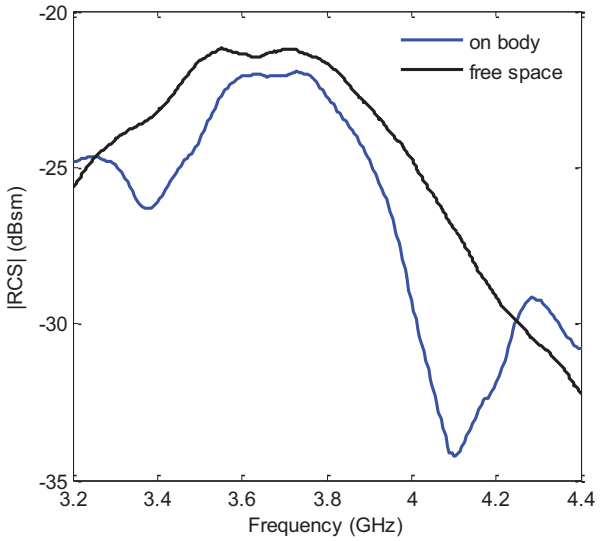

Figure 13 Measurement results for a single sewn dual rhombic loop scatterer measured in free space and on a left arm as shown in Fig. 11 (b).

VI. CONCLUSION

A concept of a sewn chipless RFID tag has been investigated. An optimized tag composed of three dual rhombic loop scatterers encoding a 3 bits capacity has been designed and optimized. The tag has been realized using a computer-aided sewing machine with electro-threads on cotton fabric. The free space measurement results in real environment, achieved with CW frequency sweep mono-static radar system, validate the design and the simulation model. The design of a chipless sensor integrated on garment has also been investigated. For this purpose, polyester stretchable fabric has been used, and a simple rectangular shaped scatterer has been realized. Several measurements carried out for various length extensions show a good correlation between the resonant frequency shift and the length extension of the scatterer in a given axis. A linear curve may approximate the measured behavior within 150 MHz frequency span. A discussion about practical issues regarding transmitting power regulations and on-body measurements gave guidelines for the next development stage of this technology in order to provide responses for mandatory requirements inherent when dealing with body-centric applications. In order to address practically identification applications, future work will focus on the way to increase the coding capacity using more efficient techniques as well as polarization diversity.

ACKNOWLEDGMENTS

This research has been funded by Finnish Funding Agency for Technology and Innovation, Academy of Finland and Centennial Foundation of Finnish Technology Industries.

REFERENCES

[1] K. Finkenzeller, “Rfid handbook: fundamentals and applications in contactless smart cards, radio frequency identification and near-field communication” *Wiley*. 2010.

[2] I. Locher, M. Klemm, T. Kirstein and G. Tröster, "Design and Characterization of Purely Textile Patch Antennas," *Advanced Packaging, IEEE Transactions on,* vol.29, no.4, pp.777-788, Nov. 2006.

[3] G. Kim;, J. Lee;, K. H. Lee;, Y. C. Chung;, J. Yeo;, B. H. Moon;, J. Yang;, and H. C. Kim;, "Design of a UHF RFID fiber tag antenna with electric-thread using a sewing machine," IEEE Microwave Conference Asia-Pacific, 16-20 Dec. 2008.

[4] Y, Kim, K. Lee, Y. Kim and Y. Chung, “Wearable UHF RFID Tag Antenna Design Using Flexible Electro-Thread and Textile,” *IEEE Antennas and Propagation Society International Symposium*, pp. 5487–5490, June 2007.

[5] J. H Choi, Y. Kim, K. Lee, and Y. Chung, “Various Wearable Embroidery RFID Tag Antennas using Electro Thread,” *IEEE International Symposium on Antennas and Propagation*, pp. 1-4, 2008.

[6] E. Moradi, T. Björninen, L. Ukkonen, Y. Rahmat-Samii, “Characterization of Embroidered Dipole-type RFID Tag Antennas,” *IEEE International Conference on RFID Technologies and Applications*, pp. 248-253, 5-7 Nov. 2012, Nice, France.

[7] E. Koski, K. Koski, T. Bjorninen, A. A. Babar, L. Sydanheimo, L. Ukkonen, and Y. Rahmat-Samii, "Fabrication of embroidered UHF RFID tags," *IEEE Antennas and Propagation Society International Symposium (APSURSI)*, 8-14 July 2012.

[8] S. Manzari, S. Pettinari and G. Marrocco, “Miniaturized and Tunable Wearable RFID Tag for Body-Centric Applications,” *IEEE International Conference on RFID Technologies and Applications*, pp. 239-244, 5-7 Nov. 2012, Nice, France.

[9] R. Saba, T. Deleruyelle, J. Alarcon, M. Egels, P. Pannier, “A Resistant Textile Tag Antenna for RFID UHF Frequency Band,” *IEEE International Conference on RFID Technologies and Applications*, pp. 203-2 07, 5-7 Nov. 2012, Nice, France.

[10] K. Koski, E. Koski, T. Bjorninen, A. A. Babar, L. Ukkonen, L. Sydanheimo and Y. Rahmat-Samii, "Practical read range evaluation of wearable embroidered UHF RFID tag," *IEEE Antennas and Propagation Society International Symposium (APSURSI),* vol., no., pp.1-2, 8-14 July 2012.

[11] Clinton S. Hartmann, “A Global SAW ID Tag with Large Data Capacity,” *IEEE Ultrasonics Symposium*, 2002, pp. 65-69.

[12] R. Nair, E. Perret & S. Tedjini, "Temporal multi-frequency encoding technique for chipless rfid applications," *Microwave Symposium Digest (MTT), 2012 IEEE MTT-S International*, pp. 1-3, 2012.

[13] I. Jalaly, D. Robertson, “RF Barcodes Using Multiple Frequency Bands,” *IEEE MTT-S International Microwave Symposium Digest*, Long Beach, CA, June 2005, pp. 139-142.

[14] J. McVay, A. Hoorfar, and N. Engheta, "Space-filling curve RFID tags," *Proc. 2006 IEEE Radio and Wireless Symp.*, San Diego, CS, pp. 17-19.

[15] S. Preradovic, N. C. Karmakar,”Multiresonator based chipless RFID tag and dedicated RFID reader,” *IEEE MTT-S International Microwave Symposium Digest*, Anaheim, CA, May 2010, pp. 1520-1523.

[16] A. Vena, E. Perret, S.Tedjini,”Chipless RFID Tag Using Hybrid Coding Technique,” *IEEE Transactions on Microwave Theory and Techniques*, Vol. 59, No 12, pp. 3356-3364, December 2011.

[17] C. Mandel, B. Kubina, M. Schüßler, and R. Jakoby, “Group-Delay Modulation with Metamaterial-Inspired Coding Particles for Passive Chipless RFID,” *IEEE International Conference on RFID Technologies and Applications*, pp. 203-207, 5-7 Nov. 2012, Nice, France.

[18] A. Vena, E. Perret, S. Tedjini, S, "A compact chipless RFID tag using polarization diversity for encoding and sensing," *IEEE International Conference on RFID*, pp.191-197, 3-5 April 2012.

[19] M.A. Islam, N.C. Karmakar, "A Novel Compact Printable Dual-Polarized Chipless RFID System," *IEEE Transactions on Microwave Theory and Techniques,* vol.60, no.7, pp.2142-2151, July 2012.

[20] IDTechEx, “Printed and Chipless RFID Forecasts, Technologies & Players 2009-2019”, www.IdtechEx.com.

[21] L. Yang, D. Staiculescu, R. Zhang, C.P. Wong, M.M. Tentzeris, "A novel “green” fully-integrated ultrasensitive RFID-enabled gas sensor utilizing inkjet-printed antennas and carbon nanotubes," *IEEE Antennas and Propagation Society International Symposium, APSURSI '09,* vol., no., pp.1 -4, 1-5 June 2009.

[22] Shieldex, USA, Yarns and fillers, datasheets available at: http://www.shieldextrading.net/yarn_and_filler.html.

[23] S. Ahmed and W. Menzel, "A novel planar four-quad antenna," 6th European Conference on Antennas and Propagation (EUCAP), pp.1946-1949, 26-30 March 2012.

[24] H. Morishita, T. Iizuka, K. Himsawa and T. Nagao, " Wideband circularly polarized rhombic loop antennas with different feed models," *IEEE Antennas and Propagation Society International Symposium*, 1995, Vol. 1, pp. 194 - 197.

[25] A. Vena, T. Singh, S. Tedjini, E. Perret, "Metallic letter identification based on radar approach," *General Assembly and Scientific Symposium, 2011 XXXth URSI*, 13-20 Aug. 2011.

[26] G. Marrocco, "Body-matched RFID antennas for wireless biometry," *First European Conference on Antennas and Propagation, EuCAP*, 6-10 Nov. 2006.